Electrospray Ionization-Induced Protein Unfolding

Hong Lin,[†] Elena N. Kitova,[†] Margaret A. Johnson,[†] Luiz Eugenio,[§] Kenneth K.S. Ng,[§] and John S. Klassen[†]

Alberta Glycomics Centre and

[†]*Department of Chemistry, University of Alberta, Edmonton, Alberta, Canada T6G 2G2*

[§]*Department of Biological Sciences, University of Calgary, Calgary, Alberta, Canada T2N 1N4*

Abstract

Electrospray ionization mass spectrometry (ESI-MS) measurements were performed under a variety of solution conditions on a highly acidic sub-fragment (B3C) of the C-terminal carbohydrate-binding repeat region of *Clostridium difficile* toxin B, and two mutants (B4A and B4B) containing fewer acidic residues. ESI-MS measurements performed in negative ion mode on aqueous ammonium acetate solutions of B3C at low ionic strength (I<80 mM) revealed evidence, based on the measured charge state distribution, of protein unfolding. In contrast, no evidence of unfolding was detected from ESI-MS measurements made in positive ion mode at low I or in either mode at higher I. The results of proton nuclear magnetic resonance and circular dichroism spectroscopy measurements and gel filtration chromatography performed on solutions of B3C under low and high I conditions suggest that the protein exists predominantly in a folded state in neutral aqueous solutions with I >10 mM. The results of ESI-MS measurements performed on B3C in a series of solutions with high I at pH 5 to 9 rule out the possibility that the structural changes are related to ESI-induced changes in pH. It is proposed that unfolding of B3C, observed in negative mode for solutions with low I, occurs during the ESI process and arises due to Coulombic repulsion between the negatively charged residues and liquid/droplet surface charge. ESI-MS measurements performed in negative ion mode on B4A and B4B also reveal a shift to higher charge states at low I but the magnitude of the changes are smaller than observed for B3C.

Introduction

Electrospray ionization mass spectrometry (ESI-MS) has become an important research tool in the fields of structural and chemical biology [1-8]. It is used to probe the higher-order structure and conformation of proteins and protein assemblies [4,6], to investigate protein folding/unfolding pathways [9-11], to identify noncovalent protein interactions and to quantify the corresponding kinetic and thermodynamic parameters [7,12-16]. The various experimental strategies available to characterize the higher-order structures of proteins and their complexes can be classified as either "direct" or "indirect" in their approach. Indirect methods typically involve ESI-MS analysis of proteolytic peptides to investigate protein conformation and interactions. For example, the extent of peptide backbone amide hydrogen-deuterium exchange can be used to interrogate the structure and dynamics of proteins and protein complexes [7,11,17]. Related and complementary approaches, based on oxidative labeling [18-19] or chemical cross-linkers [20], are also employed to deduce structural information [21]. Direct methods rely on the analysis of the intact protein or protein complex in the gas phase by ESI-MS alone or in combination with other gas phase techniques. Although the factors responsible for protein ionization in ESI are not fully understood, it is generally agreed that the size of the protein (in particular the solvent accessible surface area) is a major determining factor [22-23]. Consequently, the measured charge state distribution (CSD) can be used to establish the presence of folded and partially or fully denatured proteins in solution and to monitor conformational changes in response to changes in solution conditions [9,24-29]. Collision cross sections (CCS) of the gaseous ions of proteins and protein complexes, as determined by ion mobility spectrometry, can also provide insight into

protein structure in solution [30-32].

That the ESI process itself does not significantly perturb protein structure represents an important underlying assumption in the implementation of direct ESI-MS methods to characterize the structure of proteins and protein complexes in solution or structural changes resulting from changes to solution conditions. There exist abundant data to suggest that this is generally true. For example, the detection of noncovalent protein interactions, *e.g.*, protein-ligand and protein-protein complexes [1-7,13,15-16,33-35], by ESI-MS would not be possible if proteins were to undergo significant structural changes during the ESI process. In fact, there is growing evidence that the solution specific intermolecular interactions in protein complexes are, to some extent, preserved in the gas phase [30,33-35]. The similarities found between the CCS values measured for many gaseous protein ions and those estimated from their crystal structures also argue against widespread protein structural changes during ESI [30,36-37]. The general preservation of the native structure or close-to-native structure of proteins and protein complexes in the gas phase can be rationalized based on the timescale of the ESI process, which is typically in the μs - ms range [38-40]. Consequently, only relatively fast structural rearrangement processes will have a chance to occur during the life of the ESI droplets [41-42].

While it is generally safe to conclude, based on the abundant data described above, that protein structures and intermolecular interactions are not dramatically perturbed by the ESI process, lately evidence has emerged to show that this is not true in all situations. McLuckey and coworkers demonstrated that the charge states of gaseous protein ions formed by ESI from aqueous solutions can be significantly increased by introducing acidic or basic vapour

into the ESI source [43-45]. These observations were attributed to pH-induced changes resulting from the dissolution of the acidic or basic vapour into the ESI droplets. The addition of low-volatility reagents, such as *m*-nitrobenzyl alcohol, dimethyl sulfoxide (DMSO) and sulfolane, to aqueous protein solutions has been shown in some cases to produce a significant increase in the protein ion charge states, i.e., supercharging [41,46-48]. Williams and coworkers have attributed the increased charging to the rapid increase in reagent concentration in the ESI droplets due to solvent evaporation, which promotes thermal or chemical denaturation of the protein [48]. The hypothesis that a rapid increase in reagent concentration in the droplets promotes protein unfolding is supported by the results of a recent study by Julian and coworkers on the unfolding of myoglobin in a non-denaturing solution of water and DMSO resulting from partial lyophilization of the sample [26]. Recently, Williams and coworkers demonstrated the formation of highly charged protein ions from aqueous ammonium bicarbonate solutions at neutral pH by ESI performed in positive ion mode [49]. The enhanced charging, which was found to be sensitive to many factors including the temperature of the entrance capillary of the mass spectrometer, the spray potential and the ionic strength of the solution, was attributed to thermal denaturation of the protein resulting from the rapid heating of the ESI droplets in the atmosphere-vacuum interface [49]. Interestingly though, measurements performed on solutions containing ammonium acetate (NH_4OAc) yielded no evidence of protein unfolding.

Here, we report new evidence for protein unfolding induced by the electrospray ionization process. A series of ESI-MS measurements were performed on a highly acidic sub-fragment (B3C) of the C-terminal carbohydrate-binding repeat region of the large

exotoxin, toxin B (TcdB), produced by *Clostridium difficile* [50-51] and two mutants engineered to replace negatively charged residues with Ala residues, under a variety of solution conditions. The ESI-MS measurements performed on aqueous NH_4OAc solutions at low ionic strength (*I* <80 mM) revealed evidence, based on the measured charge state distribution, of protein unfolding in negative ion mode, but not in positive ion mode. In contrast, no evidence of unfolding was found from the ESI-MS measurements performed in either mode at high *I*. The results of proton nuclear magnetic resonance (NMR) and circular dichroism (CD) spectroscopy measurements, as well as gel filtration chromatography (GFC), performed on B3C under low and high *I* conditions indicate that the protein exists predominantly in a folded state in neutral aqueous solutions and that the structure is not strongly dependent on solution *I*. The results of control experiments confirmed that the structural changes are not related to ESI-induced changes in solution pH. It is proposed that the unfolding of B3C, which is observed in negative ion mode for solutions with low *I*, occurs in the ESI droplets and is electrostatically-driven. ESI-MS measurements performed in negative ion mode on mutants B4A and B4B, which contain fewer acidic residues than B3C, also reveal a shift to higher (negative) charge states at low *I*. However, in both cases, the magnitude of the change is smaller than observed for B3C.

Experimental section

Proteins

The TcdB-B3C fragment consists of an N-terminal Met residue, followed by six His residues and 254 residues from the carboxy-terminus of the toxin TcdB from *Clostridium difficile* strain 630 [52]. In addition to the seven non-natural residues added to the N-terminus,

two charged residues at positions 142 and 143 of B3C (Glu2246 and Lys2247 in wild-type TcdB) were replaced with Ala as a part of an unrelated study attempting to improve the crystallization properties of the protein sub-fragment. This sub-fragment from the carboxy-terminal carbohydrate-binding repeat region of TcdB contains a large excess of negatively charged residues (48 acidic Glu and Asp residues versus 13 basic Arg and Lys residues), which is characteristic of the entire repeat region.

Two artificial gene variants were also synthesized (Genscript) and cloned into the pGS-21a expression plasmid to produce two protein fragments with multiple negatively charged residues replaced by the neutral residue Ala. In B4A, Ala replaces Asp at positions 222, 224 and 244, as well as replacing Glu at positions 225, 246 and 247. B4B is identical to TcdB-B4A, except that Ala also replaces Asp at positions 109, 134 and 135, as well as replacing Glu at positions 111 and 113. However, the two charged residues (Glu at position 142 and Lys at position 143) mentioned above have been retained in the mutants rather than being replaced by Ala. As a result, B4A contains, in total, 43 acidic residues (5 fewer than B3C) while B4B contains, in total, 38 acidic residues (10 fewer than B3C). The calculated isoelectric points (*pI*) of B3C, B4A and B4B (http://web.expasy.org/protparam/) are 4.08, 4.21 and 4.32, respectively.

Each protein was expressed from a synthetic gene (Genscript) containing codons optimized for high-level expression in *Escherichia coli*. The genes were expressed from the T7 promoter in pGS-21a (Genscript) using *E. coli* C41 (DE3) as a host. Cells were grown in LB autoinduction medium (Formedium) at 26 °C for 24 h before harvesting by centrifugation, resuspension in (50 mM sodium phosphate, pH 8.0, 10 mM imidazole chloride, 300 mM

sodium chloride, 50 g/L glycerol) and stored at -80°C. The proteins were purified as previously described [52] with the addition of a final gel filtration chromatography (Sephacryl S-300 HR) step using buffer B (25 mM Tris-Cl pH 7.5, 150 mM sodium chloride, 0.5 mM EDTA, 5% (w/v) glycerol).

For the solution NMR measurements, B3C was dialyzed using Spectra/Por 4 (12-14 kDa molecular weight cut-off (MWCO)) dialysis membrane (Spectrum) for 18 h against 9.8 mM sodium/potassium phosphate buffer (pH 7.0) containing either 5 mM NaCl (low *I* sample) or 150 mM NaCl (high *I* sample). For the high *I* sample, 560 μL of protein solution was obtained and 70 μL of phosphate-buffered saline (10 mM sodium phosphate, pH 7.2, 137 mM NaCl) and 50 μL of D_2O were added to yield 680 μL of 0.3 mM B3C. For the low *I* sample, 50 μL of D_2O was added to 650 μL of protein solution to yield 700 μL of sample at 0.3 mM B3C. For the CD measurements, a series of solutions of 15 μM B3C were prepared with varying concentrations of sodium/potassium phosphate buffer to give *I* values of 20 mM, 60 mM and 105 mM. As a control, a 15 μM B3C solution containing 60 mM of sodium/potassium phosphate buffer and 6 M guanidinium chloride was also prepared and used to obtain the CD spectrum of unfolded (denatured) B3C. For the gel filtration chromatography, samples of B3C (20 μM) were dialyzed for 16 hours against each of the solutions used for gel filtration (10 mM sodium/potassium phosphate (pH 7.0) and containing 5 or 150 mM NaCl) immediately prior to injection on the column. For the ESI-MS experiments, B3C, B4A and B4B were each concentrated and exchanged with aqueous 50 mM ammonium acetate (pH 7) using ultracentrifugation microconcentrators (Millipore Corp., Bedford, MA) with a 10 kDa MWCO and stored at –20 ^{o}C if not used immediately. For all ESI-MS measurements, the

protein concentration was fixed at 15 μM. Ammonium acetate was added to the samples to yield different final concentrations ranging from 10 mM to 200 mM. The corresponding *I* values are similar in magnitude, ranging from 9.6 mM to 198.1 mM. For simplicity, the solution *I* values reported for the ESI-MS measurements are taken to be equal to ammonium acetate concentrations. Acetic acid was added for low pH solutions and ammonium hydroxide was added for high pH solutions.

Mass spectrometry measurements

In all cases, ESI was performed using nanoESI tips pulled from borosilicate glass capillaries (1.0 mm o.d., 0.78 mm i.d.) using a P-97 micropipette puller (Sutter Instruments, Novato, CA). ESI-MS measurements were performed on a Synapt G2 quadrupole-ion mobility separation-time-of-flight (Q-IMS-TOF) mass spectrometer (Waters UK Ltd., Manchester, UK) and an ApexII 9.4 tesla Fourier transform ion cyclotron resonance (FTICR) mass spectrometer (Bruker, Billerica, MA).

ApexII 9.4T FTICR mass spectrometer. Details of the standard instrumental and experimental conditions used for ESI-MS analysis of proteins with this instrument are described elsewhere [16].

Synapt G2 Q-IMS-TOF mass spectrometer. Mass spectra were obtained in either positive or negative ion modes using cesium iodide (concentration 30 ng μL^{-1}) for calibration. Given below are some of the instrumental conditions used to carry out the measurements in positive ion mode. A capillary voltage of 1.4 kV under positive mode was applied to carry out nanoESI. A cone voltage of 40 V was used and the source block temperature was maintained at 70 ºC. Other important voltages for ion transmission, that is the injection voltages into the

trap and transfer ion guides, were maintained at 10 V and 5 V, respectively. Argon was used in the trap and transfer ion guides at a pressure of 2.22 x 10^{-2} mbar and 3.36 x 10^{-2} mbar, respectively. Data acquisition and processing were carried out using MassLynx (v 4.1).

Average Charge State Calculation

The average charge state (*ACS*) of the protein ions was calculated from the ESI mass spectrum using eq 1:

$$ACS = \frac{\sum_n I_n n}{\sum_n I_n} \quad (1)$$

where I_n is the protein ion intensity (measured as peak height) and n is the charge state.

NMR measurements

1D ^{1}H NMR spectra were recorded at 21 °C on a Varian VNMRS 700 MHz spectrometer equipped with a 5mm ^{1}H{^{13}C/^{15}N} z-gradient cryogenic probe. A total of 1024 transients, consisting of 19685 complex points spanning a spectral width of 9842 Hz, were collected. The data were zero-filled to 32768 complex points and multiplied by an exponential apodization function with broadening constant of 1 Hz before Fourier transformation. The H_2O signal was suppressed using WATERGATE [53].

Circular dichroism measurements

Circular dichroism (CD) spectra were recorded at 20.8 °C on an OLIS DSM CARY-17 spectrophotometer conversion and circular dichroism module (On-line Instrument Systems Inc.) using a 0.2 mm path length quartz cuvette. Data were collected in scanning mode from 300 nm to 190 nm and the average value of 5 repetitions was reported. Data were analyzed with OLIS Spectral Works (Version 4.3), converting into molar ellipticity units. For each

buffer condition, the spectrum of the CD buffer alone was subtracted from the spectrum of the sample containing protein.

Gel filtration

Gel filtration chromatography (GFC) was performed using a Superose 6 Tricorn Column (GE Healthcare, 10 mm ID X 300 mm, 24 mL bed volume) equilibrated in 10 mM sodium/potassium phosphate (pH 7.0) and containing 5 or 150 mM NaCl. The running buffer was degassed under vacuum immediately before connecting to the chromatographic system and the column was run under a constant flow rate of 0.4 mL/min (~200 psi total system pressure) using a Shimadzu Prominence HPLC system with LC-20AD pumps and a SPD-20AV detector measuring absorbance at 280 nm. Samples of B3C (20 μM, 20 μL) were loaded onto the column using a manual injector (Rheodyne). Elution volumes and peak areas were evaluated using CLASS-VP (Shimadzu) software.

Results and Discussion

ESI mass spectra were measured in both positive and negative ion mode for aqueous solutions of B3C (15 μM) and NH_4OAc at concentrations ranging from 10 mM to 200 mM (pH 7). Shown in Figure 1 are representative mass spectra acquired in both modes for solutions containing 10 mM, 80 mM and 200 mM NH_4OAc. In all cases, the major protein ions detected correspond to multiply protonated or deprotonated B3C, i.e., $(B3C+nH)^{n+} \equiv P^{n+}$ (positive ion mode), $(B3C-nH)^{n-} \equiv P^{n-}$ (negative ion mode). Notably, the CSD observed in positive ion mode is found to be relatively insensitive to the concentration of NH_4OAc, with n ranging from +9 to +11 and an *ACS* of +10.0 ± 0.1 (Figure 2). At NH_4OAc concentrations above ~80 mM, the CSD measured in negative ion mode is similar (in terms of the number of

charges) to that observed in positive ion mode, with an *ACS* of -10.2 ± 0.1 (Figures 1c and 1d; Figure 2). However, lower NH_4OAc concentrations produce P^{n-} ions with a much broader CSD. For example at 10 mM NH_4OAc, the P^{n-} ions charge states range from -10 to -23; with a corresponding *ACS* of -16.6. The aforementioned results were acquired using the Waters Synapt G2 Q-IMS-TOF mass spectrometer. However, the present findings are independent of the instrumentation used to collect the ESI mass spectra, with similar results obtained using a 9.4T FTICR instrument (Figure S1, Supplementary Information).

The narrow CSD observed in both modes for the solutions at higher *I* suggest that B3C exists in a compact, folded form in neutral aqueous solution. However, the broadening of the CSD and shift to higher charge states observed in negative ion mode for the solutions at low *I* (< 80 mM) suggests that B3C is at least partially unfolded under these conditions. The observation of protein unfolding at low buffer concentrations (i.e., low *I*) is not, in itself, remarkable. However, it is intriguing that the ESI mass spectra acquired for the same solution, but in positive ion mode, show no evidence (based on the measured CSD) of protein unfolding. There are a number of possible explanations for these seemingly contradictory observations. It is possible that both folded and unfolded B3C co-exist in solution (at least at low *I*) and that, because of differences in relative response factors [54], ions corresponding to the unfolded protein are more abundant than those of the folded structure in negative ion mode than in positive ion mode. It also conceivable that, as reported by Kaltashov and coworkers [29], asymmetric dissociation of protein aggregates in the gas-phase alters the charge state distribution of protein ions, giving the appearance of protein unfolding in solution [55]. However, given that gentle sampling conditions (suitable for detecting

protein-ligand complexes) were employed, this explanation seems unlikely. It is also possible that unfolding occurs selectively in negative ion mode in response to an increase in the local pH of the solution at the end of the ESI tip due to electrochemical reduction of the solvent [56-57]. An alternative possibility is that the ESI process itself induces protein unfolding in the droplets, at least in negative ion mode. While it is difficult to devise experiments to directly probe protein structure or changes in structure in the droplets produced by nanoESI, it is, in principle, possible to establish the presence of different forms of B3C in bulk solution or structural changes resulting from changes in solution composition (e.g. *I*, pH).

Several lines of investigation were undertaken to establish whether B3C exists, at least in part, in an unfolded form in neutral aqueous solution at low *I*. One-dimensional (1D) ^{1}H NMR analysis was used to analyze the structure of B3C in neutral aqueous solution with low (20 mM) and high *I* (190 mM). The physical basis of the relationships between 1D NMR observables, such as chemical shift dispersion and line-width, and protein tertiary and quaternary structure are well understood [58] and are commonly used to distinguish globular (folded) proteins from partly or completely denatured proteins, natively unfolded proteins, and other intermediate folding states [59-62]. As seen in Figure 3a, the primary characteristic indicating globular folding for B3C is the high level of ^{1}H chemical shift dispersion throughout the entire spectrum, including the regions corresponding to methyl protons (−1 to 1.5 ppm), α-protons (3.5−6 ppm) and amide protons (6−10 ppm). The chemical shift dispersion in these areas results from the variety of local microenvironments created by the three-dimensional protein structure, over and above what is expected from residual structure present in unfolded polypeptide chains [63-66]. That the NMR spectra are similar under both

high and low *I* conditions suggests that the structure of B3C is not strongly influenced by *I* and that it exists predominantly in a globular form. However, due to sensitivity and signal overlap considerations, it is not possible to rule out the presence of a small fraction of unfolded protein.

The influence of *I* on the structure of B3C was also investigated by CD spectroscopy. Spectra were recorded for B3C solutions with *I* ranging from 20 mM to 105 mM (Figure 3b). Although the spectra do exhibit subtle differences over this range of *I*, the results are not consistent with a significant change in secondary structure. Furthermore, upon addition of 6 M guanidium chloride, a strong denaturant, a dramatic change in the CD spectrum is evident, consistent with the loss of ordered structure and suggesting that the majority of protein in solution is folded.

To quantitatively probe for a population of unfolded protein in solution, GFC was performed on B3C solutions with both high (190 mM) and low *I* (20 mM). Under both conditions B3C elutes almost completely in a single Gaussian-shaped peak (Figure 4). The elution volume was earlier than expected for a protein of this size, and this effect was magnified at low *I*. This effect has previously been observed in polymers bearing the same net charge as the matrix. Electrostatic repulsion between the polymer and the matrix leads to an ionic exclusion effect that reduces the effective volume available to the charged polymer, thus decreasing elution volumes relative to uncharged polymers of the same size [67]. Despite this effect, the elution volume of B3C under conditions of low or high *I* is roughly double that of the void volume, where aggregated protein with non-native three-dimensional structure is expected. Also, the lack of other significant peaks in the chromatogram strongly

indicates that unfolded forms of B3C are not present in significant amounts. Assuming that the void volume peak, which is the only significant additional peak present in the elution profile, contains unfolded protein, the total fraction of unfolded protein in the sample at either low *I* or high *I* is estimated to be <0.1%.

Taken together, the results of the NMR and CD spectroscopy and GFC measurements suggest that B3C exists predominantly in a folded state in neutral aqueous solutions with *I* values of 20 to 190 mM. It follows then, that the differences in CSD observed for B3C in negative ion mode ESI-MS under low and high *I* conditions do not reflect protein structural changes in bulk solution.

If the differences in CSD observed in positive and negative ion mode for the solutions with low *I* do not reflect the presence of both folded and unfolded B3C in bulk solution (and differences in relative response factors), then the differences must be due to the ESI process itself. To establish whether the unfolding of B3C occurs selectively in negative ion mode (for solutions with low *I*) due to an electrochemically-induced increase in the local pH at the end of the ESI tip, ESI-MS measurements were performed on aqueous solutions of B3C with high *I* (200 mM) at pH values ranging from 5 to 9 in both positive and negative ion modes (Figure 5). Although there are subtle differences in the appearance of the mass spectra measured for the solutions at different pH values, in particular the extent of adduct formation observed in negative ion mode, the CSD of the B3C ions exhibits no significant dependence on the solution pH in either mode. These results conclusively rule out the possibility that changes in pH are responsible for the differences in CSD observed in negative ion mode for solutions of B3C at low and high *I*.

If pH changes are not responsible for the difference in the CSD measured for B3C in at low and high *I* in negative ion mode then one is forced to consider the possibility that unfolding occurs selectively during the ESI process carried out in negative ion mode, albeit only for solutions at low *I*. But what is the driving force for unfolding? B3C is an unusually acidic protein and is expected to have high surface activity owing to the large excess of negative charge present at neutral pH. Consequently, it is conceivable that Coulombic repulsion between the negatively charged residues and the ESI droplet surface charge induces unfolding. That unfolding is not observed in negative ion mode for solutions with higher *I* can be attributed to the effective shielding of the negative charges by the buffer ions. It has been shown in a number of studies that proteins in aqueous solution can be denatured by relatively high electric fields [68-70]. Therefore, it is also possible that unfolding occurs at the ESI tip prior to droplet formation.

To test the hypothesis that B3C undergoes charge-induced unfolding in negative ion mode, ESI-MS measurements were performed on neutral aqueous solutions of two mutant proteins, B4A and B4B, which have fewer (5 and 10, respectively) acidic residues than B3C, and NH_4OAc concentrations ranging from 10 to 200 mM. Illustrative mass spectra acquired in both modes for solutions containing 15 μM mutant protein and NH_4OAc at three different concentrations are shown for B4A and B4B in Figure S2 and S3, respectively. The corresponding plots of *ACS* versus *I* are shown in Figure 6. It can be seen that for both mutants the mass spectra acquired for solutions with low and high *I* are qualitatively similar to those measured for B3C (Figure 1). For solutions with high *I*, the *ACS* measured for B4A and B4B in positive and negative ion modes (10.6 ± 0.1 and -10.6 ± 0.1, and 10.6 ± 0.1 and

-10.3 ± 0.3, respectively) are similar to the results obtained for B3C. For the solutions at low *I* (10 mM) there is no evidence of unfolding in positive ion mode. In contrast, in negative ion mode the *ACS* increases significantly, to -14.0 for B4A and -12.7 for B4B, which is consistent with unfolding. However, the absolute *ACS* values determined under these conditions are noticeably smaller than those measured for B3C. Furthermore, inspection of the plot of *ACS* versus *I* reveals that the onset of unfolding for the two mutants occurs at lower NH_4OAc concentrations than found for B3C. For B4A, the *ACS* values start to increase (become more negative) at concentrations <60 mM, while for B4B the change occurs at concentrations <40 mM. These differences are more clearly seen in the mass spectra measured for B3C, B4A and B4B at NH_4OAc concentrations of 20 mM, 40 mM and 60 mM (Figures S4, S5 and S6). That the increase in *ACS* in negative ion mode occurs at lower *I* is consistent with the reduction in the electrostatic repulsion (the putative driving force for protein unfolding) between the mutant proteins, which contain fewer acidic residues, and the droplet surface charge.

Conclusions

The results of the present study provide evidence for the occurrence of rapid, electrostatic-induced unfolding of acidic proteins in negatively charged ESI droplets. The extent of unfolding of the recombinant fragments B3C, B4A and B4B of TcdB in negative ion mode ESI-MS, which was monitored by changes in the CSD and the *ACS*, was found to be sensitive to the concentration of the solution "buffer", NH_4OAc. For neutral solutions of B3C at high *I*, >80 mM, the mass spectra exhibit a relatively narrow CSD and constant *ACS*, consistent with the protein having a compact structure. However, for solutions at lower *I*, the proteins exhibit a much broader CSD and a substantially larger (absolute) *ACS*, consistent

with unfolding of the protein. In contrast, the CSD and *ACS* measured in positive ion mode are essentially independent of *I* (over the range investigated) and consistent with a folded protein. The results of ^{1}H NMR and CD spectroscopy and GFC measurements performed on solutions of B3C under low and high *I* conditions also suggest that the protein exists predominantly in a folded state in neutral aqueous solutions with *I* >10 mM. The results of ESI-MS measurements performed on a series of solutions of B3C with high *I* at pH 5 to 9 ruled out the possibility that the structural changes are related to ESI-induced changes in solution pH. Instead, it is proposed that the unfolding of B3C, observed in negative mode for solutions with low *I*, occurs in the ESI droplets and arises due to Coulombic repulsion between the negatively charged residues of the protein and droplet surface charge. The results of ESI-MS measurements performed on the mutants B4A and B4B, which contain fewer acidic residues than B3C, also reveal a shift to higher absolute *ACS* at low *I*. However, in both cases the magnitude of the change is smaller than observed for B3C, consistent with the proposed electrostatic-induced unfolding mechanism.

Acknowledgement

The authors acknowledge the Natural Sciences and Engineering Research Council of Canada and the Alberta Glycomics Centre for funding.

References

1. Smith, R.D., Loo, J.A., Edmonds, C.G., Barinaga, C.J., Udseth, H.R.: New developments in biochemical mass spectrometry: electrospray ionization. *Anal. Chem.* **62,** 882-899 (1990)

2. Loo, J.A.: Studying noncovalent protein complexes by electrospray ionization mass spectrometry. *Mass Spectrom. Rev.* **16,** 1-23 (1997)

3. Loo, J.A.: Electrospray ionization mass spectrometry: a technology for studying noncovalent macromolecular complexes. *Int. J. Mass spectrom.* **200,** 175-186 (2000)

4. Benesch, J.L.P., Robinson, C.V.: Mass spectrometry of macromolecular assemblies: preservation and dissociation. *Curr. Opin. Struct. Biol.* **16,** 245-251 (2006)

5. Heck, A.J.R.: Native mass spectrometry: a bridge between interactomics and structural biology. *Nat Meth* **5,** 927-933 (2008)

6. Heck, A.J.R., van den Heuvel, R.H.H.: Investigation of intact protein complexes by mass spectrometry. *Mass Spectrom. Rev.* **23,** 368-389 (2004)

7. Konermann, L., Pan, J., Liu, Y.-H.: Hydrogen exchange mass spectrometry for studying protein structure and dynamics. *Chem. Soc. Rev.* **40,** 1224-1234 (2011)

8. Sharon, M., Robinson, C.V.: The Role of Mass Spectrometry in Structure Elucidation of Dynamic Protein Complexes. *Annu. Rev. Biochem* **76,** 167-193 (2007)

9. Konermann, L., Douglas, D.J.: Equilibrium unfolding of proteins monitored by electrospray ionization mass spectrometry: distinguishing two-state from multi-state transitions. *Rapid Commun. Mass Spectrom.* **12,** 435-442 (1998)

10. Kaltashov, I.A., Eyles, S.J.: Studies of biomolecular conformations and conformational dynamics by mass spectrometry. *Mass Spectrom. Rev.* **21,** 37-71 (2002)

11. Konermann, L., Tong, X., Pan, Y.: Protein structure and dynamics studied by mass spectrometry: H/D exchange, hydroxyl radical labeling, and related approaches. *J. Mass Spectrom.* **43,** 1021-1036 (2008)

12. Powell, K.D., Ghaemmaghami, S., Wang, M.Z., Ma, L., Oas, T.G., Fitzgerald, M.C.: A General Mass Spectrometry-Based Assay for the Quantitation of Protein−Ligand Binding Interactions in Solution. *J. Am. Chem. Soc.* **124,** 10256-10257 (2002)

13. Shoemaker, G.K., Kitova, E.N., Klassen, J.S.: Protein-Carbohydrate Affinities: An Example of a Direct Method to Determine Equilitrium Constants. *The Encyclopedia of Mass Spectrometry* **6,** 810-822 (2006)

14. Konermann, L., Simmons, D.A.: Protein-folding kinetics and mechanisms studied by pulse-labeling and mass spectrometry. *Mass Spectrom. Rev.* **22,** 1-26 (2003)

15. Kitova, E., El-Hawiet, A., Schnier, P., Klassen, J.: Reliable Determinations of Protein–Ligand Interactions by Direct ESI-MS Measurements. Are We There Yet? *J. Am. Soc. Mass Spectrom.* **23,** 431-441 (2012)

16. Liu, L., Kitova, E., Klassen, J.: Quantifying Protein-Fatty Acid Interactions Using Electrospray Ionization Mass Spectrometry. *J. Am. Soc. Mass Spectrom.* **22,** 310-318 (2011)

17. Marcsisin, S., Engen, J.: Hydrogen exchange mass spectrometry: what is it and what can it tell us? *Anal. Bioanal. Chem.* **397,** 967-972 (2010)

18. Zhang, H., Gau, B.C., Jones, L.M., Vidavsky, I., Gross, M.L.: Fast photochemical oxidation of proteins for comparing structures of protein-ligand complexes: The calmodulin-peptide model system. *Anal. Chem.* **83,** 311-318 (2011)

19. Pan, Y., Ruan, X., Valvano, M., Konermann, L.: Validation of Membrane Protein

Topology Models by Oxidative Labeling and Mass Spectrometry. *J. Am. Soc. Mass Spectrom.* **23,** 889-898 (2012)

20. Sohn, C.H., Agnew, H.D., Lee, J.E., Sweredoski, M.J., Graham, R.L.J., Smith, G.T., Hess, S., Czerwieniec, G., Loo, J.A., Heath, J.R., Deshaies, R.J., Beauchamp, J.L.: Designer reagents for mass spectrometry-based proteomics: Clickable cross-linkers for elucidation of protein structures and interactions. *Anal. Chem.* **84,** 2662-2669 (2012)

21. Sinz, A.: Chemical cross-linking and mass spectrometry to map three-dimensional protein structures and protein-protein interactions. *Mass Spectrom. Rev.* **25,** 663-682 (2006)

22. Kaltashov, I.A., Mohimen, A.: Estimates of Protein Surface Areas in Solution by Electrospray Ionization Mass Spectrometry. *Anal. Chem.* **77,** 5370-5379 (2005)

23. Testa, L., Brocca, S., Grandori, R.: Charge-Surface Correlation in Electrospray Ionization of Folded and Unfolded Proteins. *Anal. Chem.* **83,** 6459-6463 (2011)

24. Chowdhury, S.K., Katta, V., Chait, B.T.: Probing conformational changes in proteins by mass spectrometry. *J. Am. Chem. Soc.* **112,** 9012-9013 (1990)

25. Grandori, R.: Origin of the conformation dependence of protein charge-state distributions in electrospray ionization mass spectrometry. *J. Mass Spectrom.* **38,** 11-15 (2003)

26. Hamdy, O., Julian, R.: Reflections on Charge State Distributions, Protein Structure, and the Mystical Mechanism of Electrospray Ionization. *J. Am. Soc. Mass Spectrom.* **23,** 1-6 (2012)

27. Hall, Z., Robinson, C.V.: Do Charge State Signatures Guarantee Protein Conformations? *J. Am. Soc. Mass Spectrom.* 1-8 (2012)

28. Konermann, L., Douglas, D.: Unfolding of proteins monitored by electrospray ionization

mass spectrometry: a comparison of positive and negative ion modes. *J. Am. Soc. Mass Spectrom.* **9,** 1248-1254 (1998)

29. Kaltashov, I.A., Abzalimov, R.R.: Do Ionic Charges in ESI MS Provide Useful Information on Macromolecular Structure? *J. Am. Soc. Mass Spectrom.* **19,** 1239-1246 (2008)

30. Ruotolo, B.T., Giles, K., Campuzano, I., Sandercock, A.M., Bateman, R.H., Robinson, C.V.: Evidence for Macromolecular Protein Rings in the Absence of Bulk Water. *Science* **310,** 1658-1661 (2005)

31. Zhong, Y., Hyung, S.J., Ruotolo, B.T.: Ion mobility-mass spectrometry for structural proteomics. *Expert Rev Proteomics* **9,** 47-58 (2012)

32. Duijn, E.v., Barendregt, A., Synowsky, S., Versluis, C., Heck, A.J.R.: Chaperonin Complexes Monitored by Ion Mobility Mass Spectrometry. *J. Am. Chem. Soc.* **131,** 1452-1459 (2009)

33. Kitova, E.N., Bundle, D.R., Klassen, J.S.: Evidence for the Preservation of Specific Intermolecular Interactions in Gaseous Protein−Oligosaccharide Complexes. *J. Am. Chem. Soc.* **124,** 9340-9341 (2002)

34. Kitova, E.N., Seo, M., Roy, P.-N., Klassen, J.S.: Elucidating the Intermolecular Interactions within a Desolvated Protein−Ligand Complex. An Experimental and Computational Study. *J. Am. Chem. Soc.* **130,** 1214-1226 (2008)

35. Liu, L., Bagal, D., Kitova, E.N., Schnier, P.D., Klassen, J.S.: Hydrophobic Protein−Ligand Interactions Preserved in the Gas Phase. *J. Am. Chem. Soc.* **131,** 15980-15981 (2009)

36. Scarff, C.A., Thalassinos, K., Hilton, G.R., Scrivens, J.H.: Travelling wave ion mobility

mass spectrometry studies of protein structure: biological significance and comparison with X-ray crystallography and nuclear magnetic resonance spectroscopy measurements. *Rapid Commun. Mass Spectrom.* **22,** 3297-3304 (2008)

37. Jurneczko, E., Barran, P.E.: How useful is ion mobility mass spectrometry for structural biology? The relationship between protein crystal structures and their collision cross sections in the gas phase. *Analyst* **136,** 20-28 (2011)

38. Mirza, U.A., Chait, B.T.: Do proteins denature during droplet evolution in electrospray ionization? *Int. J. Mass Spectrom. Ion Processes* **162,** 173-181 (1997)

39. Breuker, K., McLafferty, F.W.: Stepwise evolution of protein native structure with electrospray into the gas phase, 10^{-12} to 10^{2} s. *Proc. Natl. Acad. Sci. U.S.A.* **105,** 18145-18152 (2008)

40. Wyttenbach, T., Bowers, M.T.: Structural Stability from Solution to the Gas Phase: Native Solution Structure of Ubiquitin Survives Analysis in a Solvent-Free Ion Mobility–Mass Spectrometry Environment. *J. Phys. Chem. B* **115,** 12266-12275 (2011)

41. Sterling, H., Prell, J., Cassou, C., Williams, E.: Protein Conformation and Supercharging with DMSO from Aqueous Solution. *J. Am. Soc. Mass Spectrom.* **22,** 1178-1186 (2011)

42. Di Marco, V.B., Bombi, G.G.: Electrospray mass spectrometry (ESI-MS) in the study of metal–ligand solution equilibria. *Mass Spectrom. Rev.* **25,** 347-379 (2006)

43. Kharlamova, A., Prentice, B.M., Huang, T.-Y., McLuckey, S.A.: Electrospray Droplet Exposure to Gaseous Acids for the Manipulation of Protein Charge State Distributions. *Anal. Chem.* **82,** 7422-7429 (2010)

44. Kharlamova, A., DeMuth, J., McLuckey, S.: Vapor Treatment of Electrospray Droplets:

Evidence for the Folding of Initially Denatured Proteins on the Sub-Millisecond Time-Scale. *J. Am. Soc. Mass Spectrom.* **23,** 88-101 (2012)

45. Kharlamova, A., McLuckey, S.A.: Negative Electrospray Droplet Exposure to Gaseous Bases for the Manipulation of Protein Charge State Distributions. *Anal. Chem.* **83,** 431-437 (2011)

46. Iavarone, A.T., Jurchen, J.C., Williams, E.R.: Supercharged Protein and Peptide Ions Formed by Electrospray Ionization. *Anal. Chem.* **73,** 1455-1460 (2001)

47. Sterling, H., Daly, M., Feld, G., Thoren, K., Kintzer, A., Krantz, B., Williams, E.: Effects of supercharging reagents on noncovalent complex structure in electrospray ionization from aqueous solutions. *J. Am. Soc. Mass Spectrom.* **21,** 1762-1774 (2010)

48. Sterling, H., Williams, E.: Origin of supercharging in electrospray ionization of noncovalent complexes from aqueous solution. *J. Am. Soc. Mass Spectrom.* **20,** 1933-1943 (2009)

49. Sterling, H.J., Cassou, C.A., Susa, A.C., Williams, E.R.: Electrothermal Supercharging of Proteins in Native Electrospray Ionization. *Anal. Chem.* **84,** 3795-3801 (2012)

50. Voth, D.E., Ballard, J.D.: Clostridium difficile Toxins: Mechanism of Action and Role in Disease. *Clin. Microbiol. Rev.* **18,** 247-263 (2005)

51. Curry, S.R., Marsh, J.W., Muto, C.A., O'Leary, M.M., Pasculle, A.W., Harrison, L.H.: tcdC Genotypes Associated with Severe TcdC Truncation in an Epidemic Clone and Other Strains of Clostridium difficile. *J. Clin. Microbiol.* **45,** 215-221 (2007)

52. Ho, J.G.S., Greco, A., Rupnik, M., Ng, K.K.-S.: Crystal structure of receptor-binding C-terminal repeats from Clostridium difficile toxin A. *Proc. Natl. Acad. Sci. U.S.A.* **102,**

18373-18378 (2005)

53. Piotto, M., Saudek, V., Sklenář, V.: Gradient-tailored excitation for single-quantum NMR spectroscopy of aqueous solutions. *J. Biomol. NMR* **2,** 661-665 (1992)

54. Kuprowski, M.C., Konermann, L.: Signal Response of Coexisting Protein Conformers in Electrospray Mass Spectrometry. *Anal. Chem.* **79,** 2499-2506 (2007)

55. Abzalimov, R.R., Frimpong, A.K., Kaltashov, I.A.: Gas-phase processes and measurements of macromolecular properties in solution: On the possibility of false positive and false negative signals of protein unfolding. *Int. J. Mass spectrom.* **253,** 207-216 (2006)

56. Van Berkel, G., Asano, K., Schnier, P.: Electrochemical processes in a wire-in-a-capillary bulk-loaded, nano-electrospray emitter. *J. Am. Soc. Mass Spectrom.* **12,** 853-862 (2001)

57. Wang, W., Kitova, E.N., Klassen, J.S.: Influence of Solution and Gas Phase Processes on Protein−Carbohydrate Binding Affinities Determined by Nanoelectrospray Fourier Transform Ion Cyclotron Resonance Mass Spectrometry. *Anal. Chem.* **75,** 4945-4955 (2003)

58. Wüthrich, K.: NMR of Proteins and Nucleic Acids. (1986)

59. Page, R., Peti, W., Wilson, I.A., Stevens, R.C., Wüthrich, K.: NMR screening and crystal quality of bacterially expressed prokaryotic and eukaryotic proteins in a structural genomics pipeline. *Proc. Natl. Acad. Sci. U.S.A.* **102,** 1901-1905 (2005)

60. Hill, J.M.: NMR screening for rapid protein characterization in structural proteomics. *Methods Mol. Biol. (Clifton, N.J.)* **426,** 437-446 (2008)

61. Rehm, T., Huber, R., Holak, T.A.: Application of NMR in Structural Proteomics: Screening for Proteins Amenable to Structural Analysis. *Structure* **10,** 1613-1618 (2002)

62. Peti, W., Etezady-Esfarjani, T., Herrmann, T., Klock, H.E., Lesley, S.A., Wüthrich, K.:

NMR for structural proteomics of Thermotoga maritima: Screening and structure determination. *J. Struct. Funct. Genomics* **5,** 205-215 (2004)

63. Neri, D., Billeter, M., Wider, G., Wuthrich, K.: NMR determination of residual structure in a urea-denatured protein, the 434-repressor. *Science* **257,** 1559-1563 (1992)

64. Neri, D., Wider, G., Wuthrich, K.: Complete 15N and 1H NMR assignments for the amino-terminal domain of the phage 434 repressor in the urea-unfolded form. *Proc. Natl. Acad. Sci. U.S.A.* **89,** 4397-4401 (1992)

65. Tafer, H., Hiller, S., Hilty, C., Fernández, C., Wüthrich, K.: Nonrandom Structure in the Urea-Unfolded Escherichia coli Outer Membrane Protein X (OmpX). *Biochemistry* **43,** 860-869 (2004)

66. Eliezer, D.: Characterizing residual structure in disordered protein States using nuclear magnetic resonance. *Methods Mol. Biol. (Clifton, N.J.)* **350,** 49-67 (2007)

67. Mori, S.: Secondary effects in aqueous size exclusion chromatography of sodium poly(styrene sulfonate) compounds. *Anal. Chem.* **61,** 530-534 (1989)

68. Xu, D., Phillips, J.C., Schulten, K.: Protein Response to External Electric Fields: Relaxation, Hysteresis, and Echo. *J. Phys. Chem.* **100,** 12108-12121 (1996)

69. Talaga, D.S., Li, J.: Single-Molecule Protein Unfolding in Solid State Nanopores. *J. Am. Chem. Soc.* **131,** 9287-9297 (2009)

70. Wu, T., Bur, A., Wong, K., Hockel, J.L., Hsu, C.J., Kim, H.K.D., Wang, K.L., Carman, G.P.: Electric-poling-induced magnetic anisotropy and electric-field-induced magnetization reorientation in magnetoelectric Ni/(011) $[Pb(Mg_{1/3}Nb_{2/3})O_3]_{(1-x)}$-$[PbTiO_3]_x$ heterostructure. *J. Appl. Phys.* **109,** (2011)

Figure captions

Figure 1 ESI mass spectra acquired in positive ion mode for aqueous solutions of TcdB-B3C (P, 15 μM) and ammonium acetate (a) 10 mM, (c) 80 mM and (e) 200 mM. ESI mass spectra acquired in negative ion mode for aqueous solutions of TcdB-B3C (P, 15 μM) and ammonium acetate (b) 10 mM, (d) 80 mM and (f) 200 mM

Figure 2 Plot of average charge state (*ACS*) versus ionic strength (*I*) measured from ESI mass spectra acquired in positive (■) and negative (●) ion modes for aqueous ammonium acetate solutions (pH 7) of TcdB-B3C (15 μM)

Figure 3 (a) 1D ^{1}H NMR spectra for neutral aqueous solutions of TcdB-B3C. The spectrum shown in black was measured with 0.3 mM B3C in phosphate buffer (pH 7.0) with 150 mM NaCl. The spectrum shown in red was measured with 0.3 mM B3C in phosphate buffer (pH 7.0) with 5 mM NaCl. The spectra were recorded at 21 °C, with 1024 scans and with WATERGATE water suppression [53], on a Varian VNMRS 700 MHz spectrometer equipped with a 5mm ^{1}H{^{13}C/^{15}N} z-gradient cryogenic probe. The sharp lines between 3.2 and 3.6 ppm derive from the concentrator membrane. (b) CD spectra of aqueous solutions of TcdB-B3C with phosphate buffer at different ionic strengths: 20 mM, ■; 60 mM, ●; 105 mM, ▲; and with the addition of 6 M guanidinium chloride, ♦.

Figure 4 Chromatograms of B3C (12 μg) eluted from Superose 6 10/300 gel filtration column equilibrated with 10 mM sodium/potassium phosphate (pH 7.0) and (a)

5 mM sodium chloride or (b) 150 mM sodium chloride. The inset in panel (a) shows a magnified view of the void volume peak.

Figure 5 ESI mass spectra acquired in positive ion mode for aqueous solutions of TcdB-B3C (P, 15 μM) and ammonium acetate (200 mM) at pH (a) 9.0, (b) 8.0, (c) 7.0, (d) 6.0 and (e) 5.0. ESI mass spectra acquired in negative ion mode for aqueous solutions of TcdB-B3C (P, 15 μM) and ammonium acetate (200 mM) at pH (f) 9.0, (g) 8.0, (h) 7.0, (i) 6.0 and (j) 5.0.

Figure 6 Plots of average charge state (*ACS*) versus ionic strength (*I*) measured from ESI mass spectra acquired in positive (■) and negative (●) ion mode for aqueous ammonium acetate solutions (pH 7) of two mutants (a) TcdB-B4A (10 μM) and (b) TcdB-B4B (10 μM). The ESI-MS measurements were carried out using identical instrumental/experimental conditions as those used for TcdB-B3C.

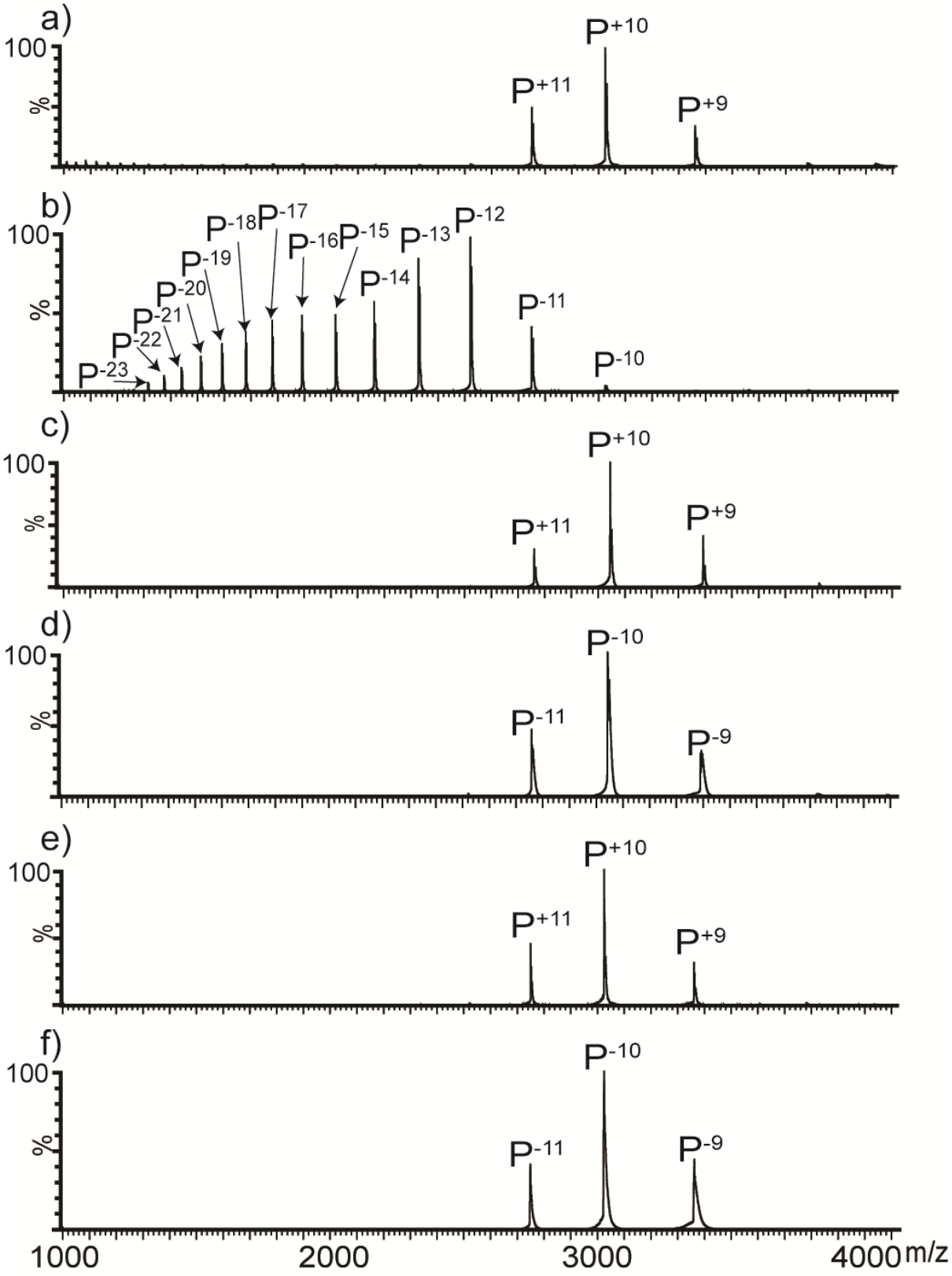
a)
100
%
P+10
P+11
P+9
b)
100
%
P-18
P-17
P-16
P-15
P-19
P-20
P-21
P-22
P-23
P-14
P-13
P-12
P-11
P-10
c)
100
%
P+10
P+11
P+9
d)
100
%
P-10
P-11
P-9
e)
100
%
P+10
P+11
P+9
f)
100
%
P-10
P-11
P-9
1000
2000
3000
4000
m/z

Fig. 1

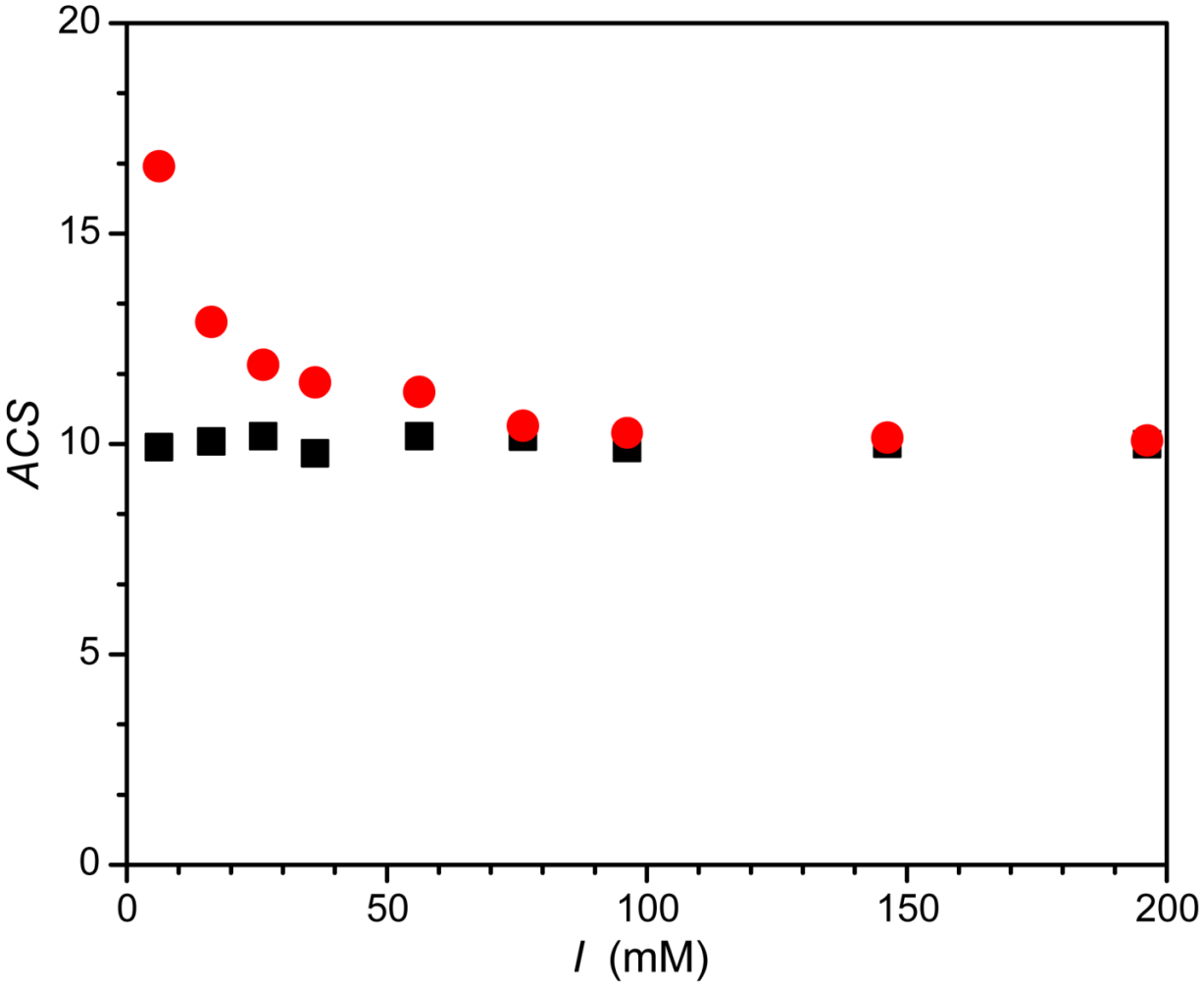

Fig. 2

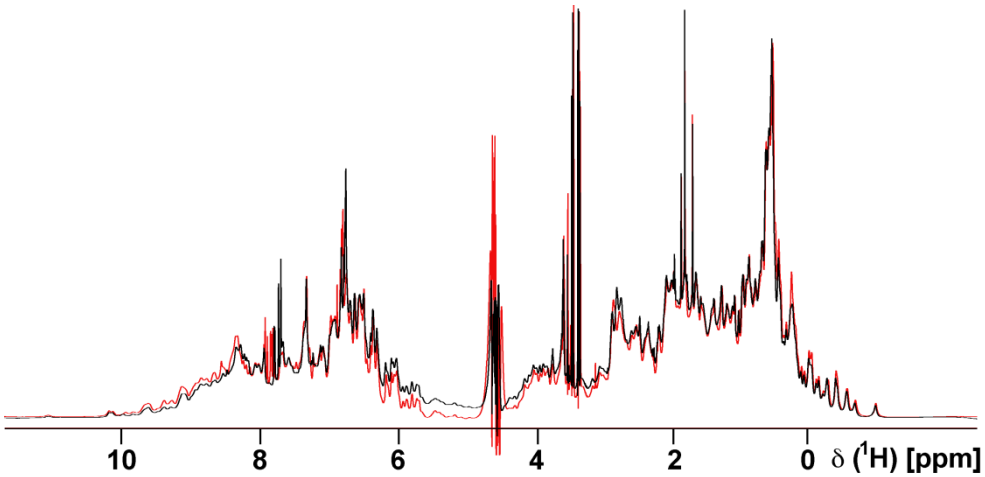

Fig. 3

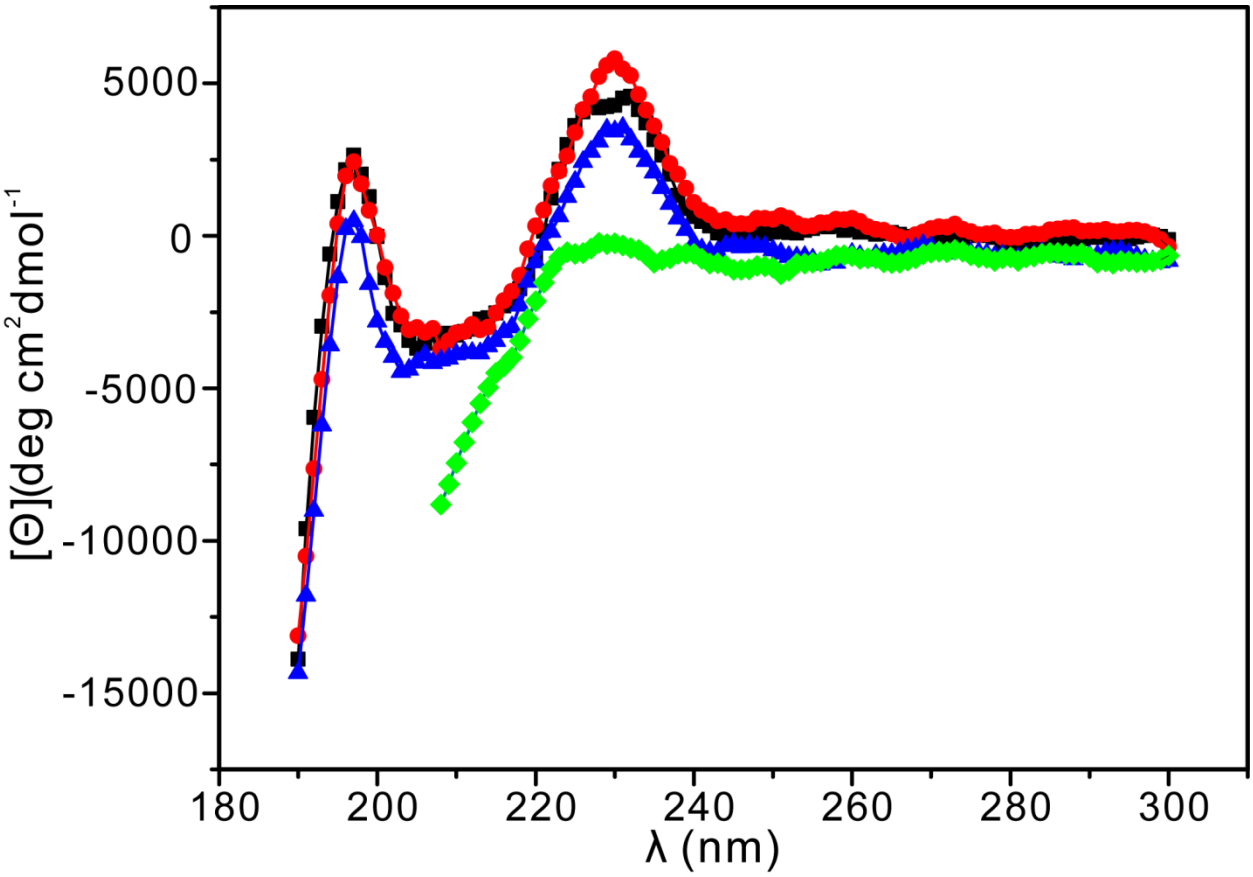
5000
0
-5000
-10000
-15000
[Θ](deg cm2dmol-1
180
200
220
240
260
280
300
λ (nm)

Fig. 4

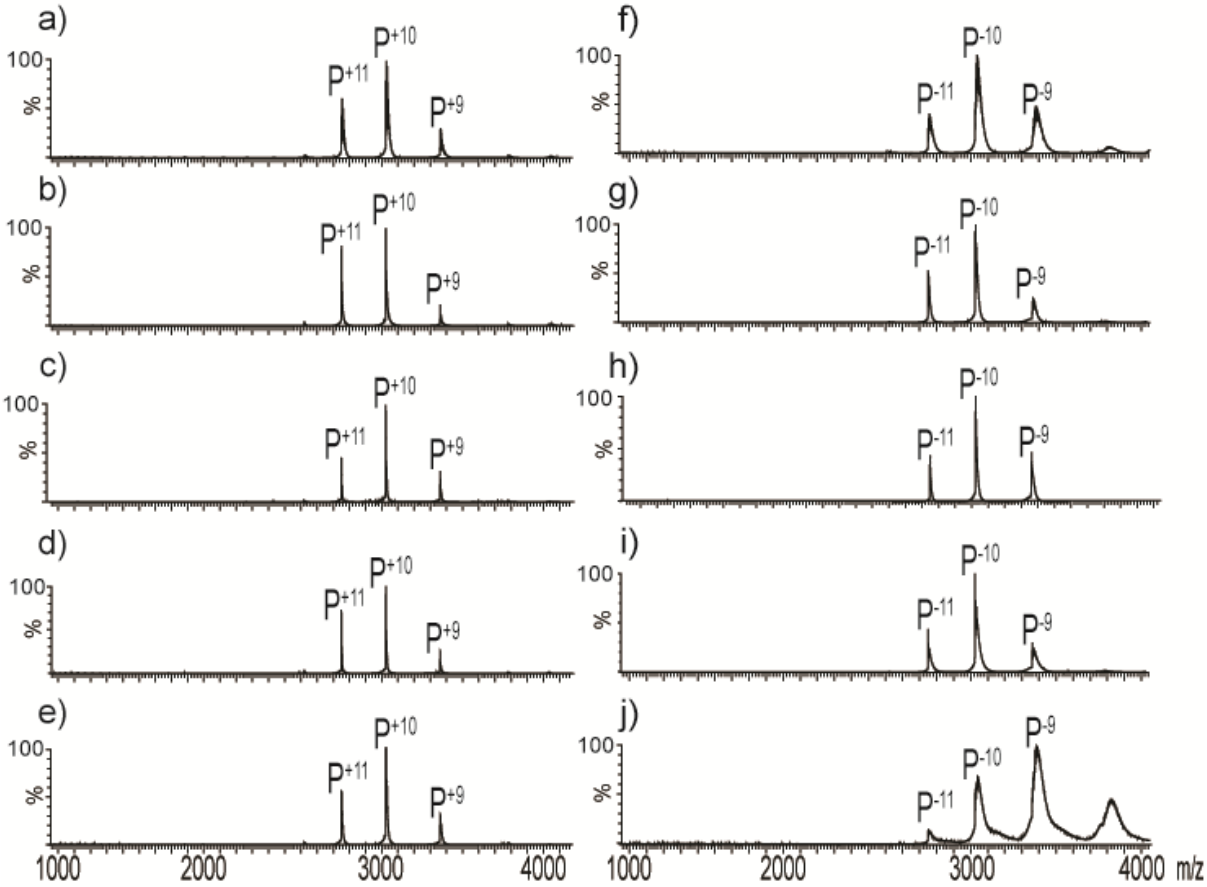

Fig. 5

a)

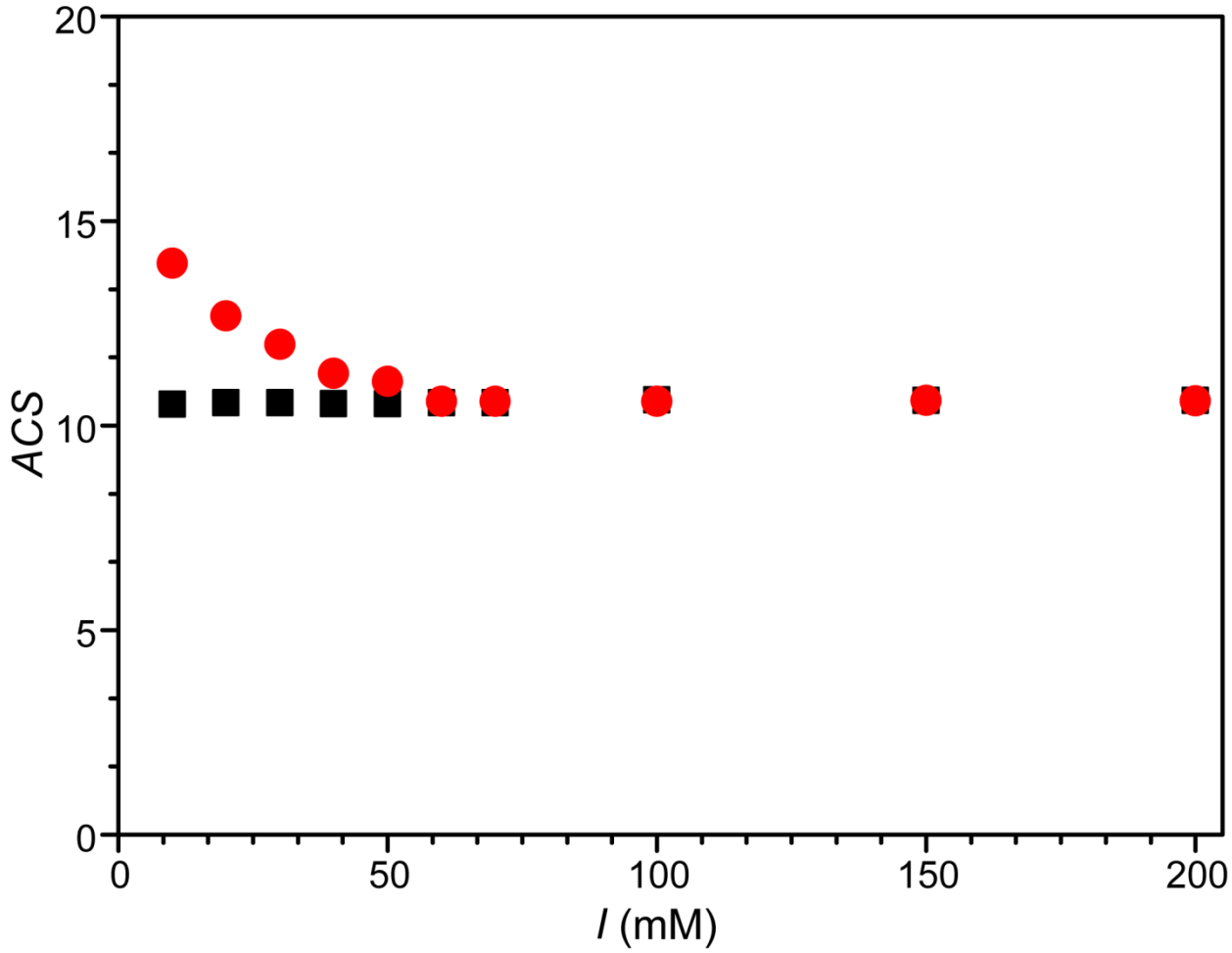

b)

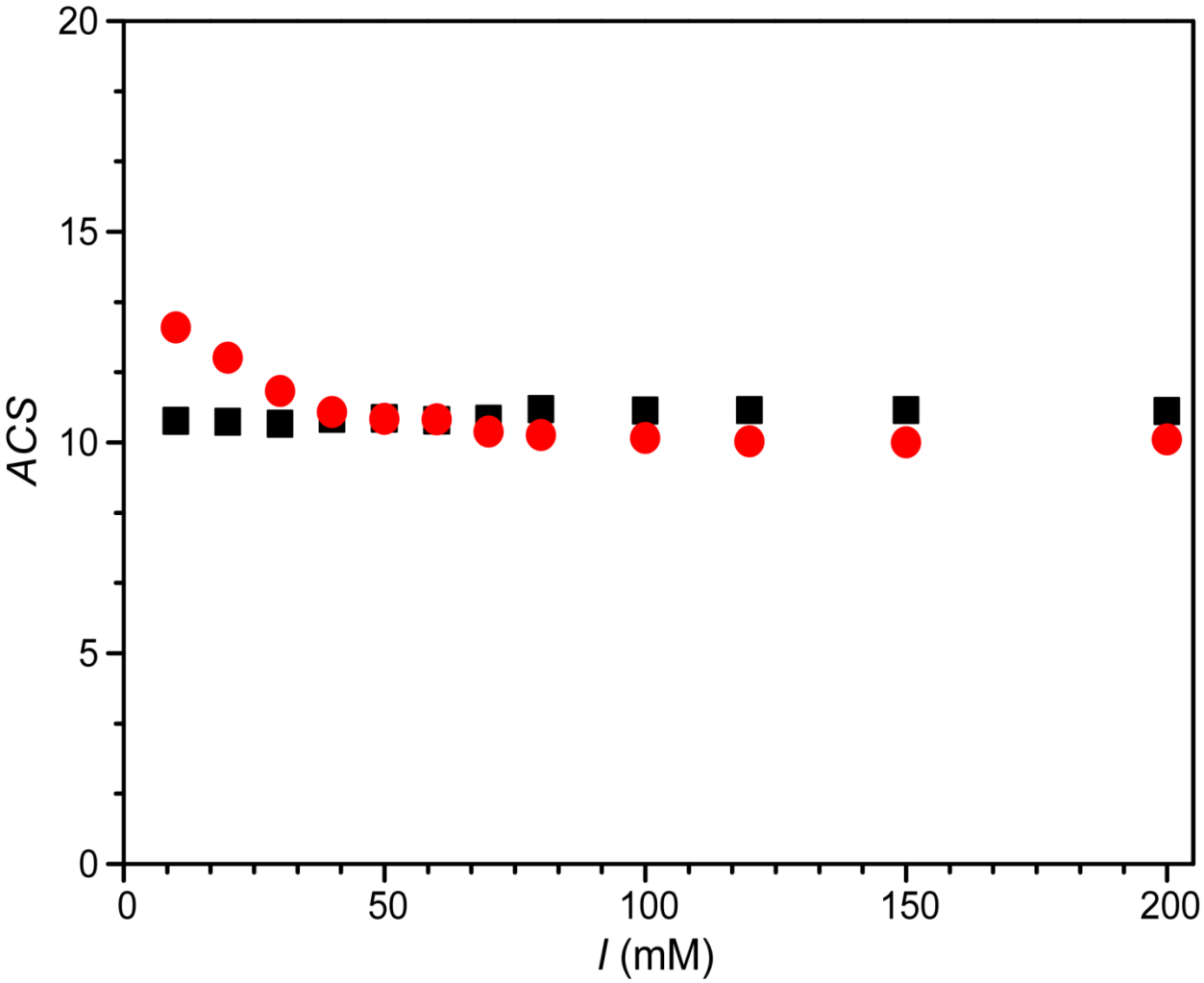

Fig. 6

a)

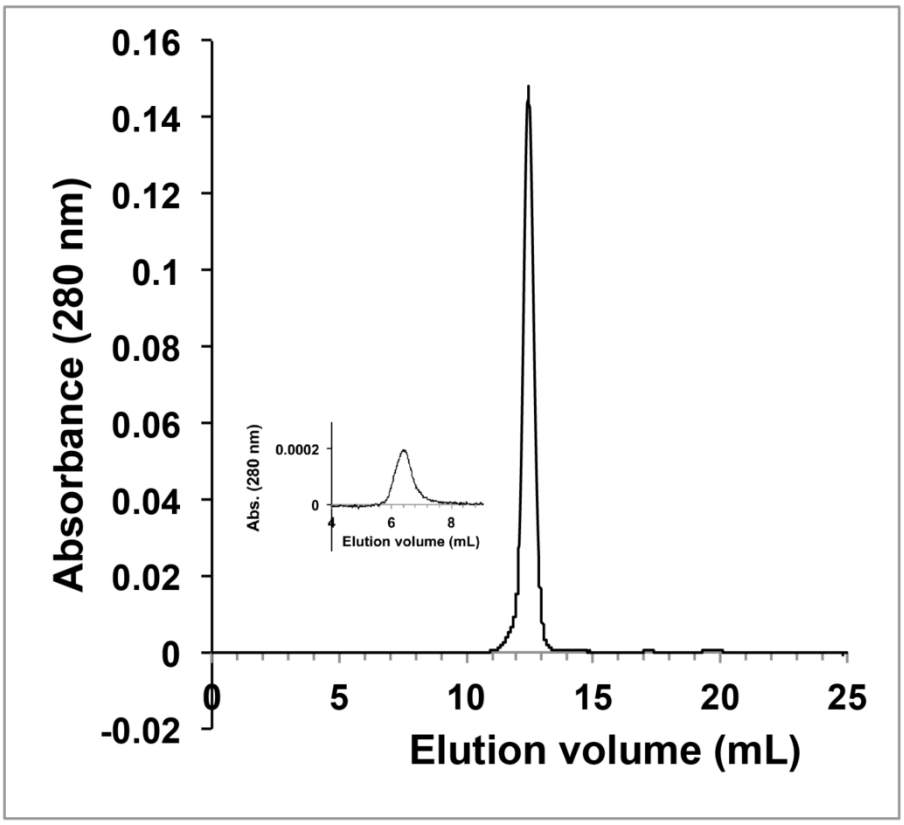
0.16
0.14
0.12
0.1
0.08
0.06
0.04
0.02
0
-0.02
Absorbance (280 nm)
0
5
10
15
20
25
Elution volume (mL)
Abs. (280 nm)
0.0002
0
4
6
8
Elution volume (mL)

b)

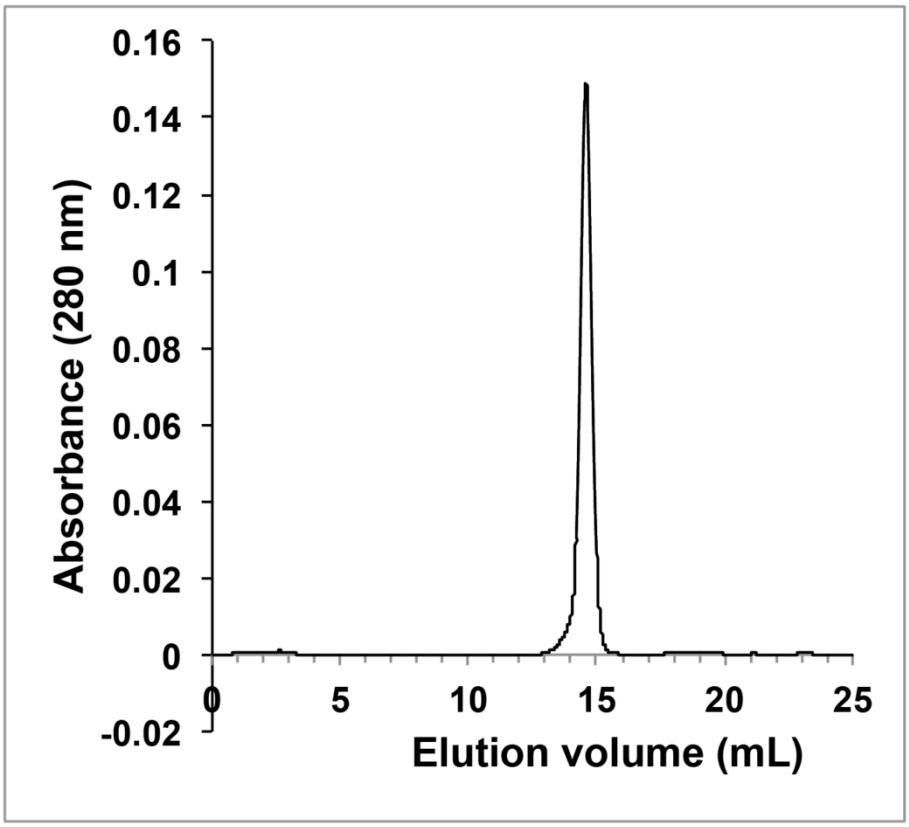
0.16
0.14
0.12
0.1
0.08
0.06
0.04
0.02
0
-0.02
Absorbance (280 nm)
0
5
10
15
20
25
Elution volume (mL)

Fig. X

Graphical abstract

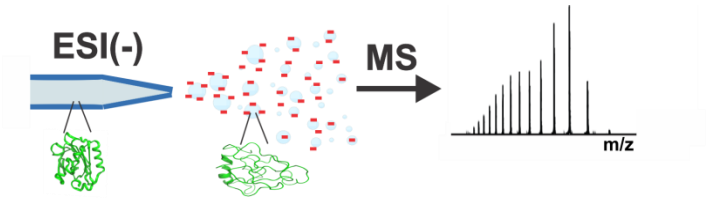

Supplementary Information for:

Electrospray Ionization-Induced Protein Unfolding

Hong Lin, Elena N. Kitova, Margaret A. Johnson, Luiz Eugenio, Kenneth K.S. Ng, and John S. Klassen

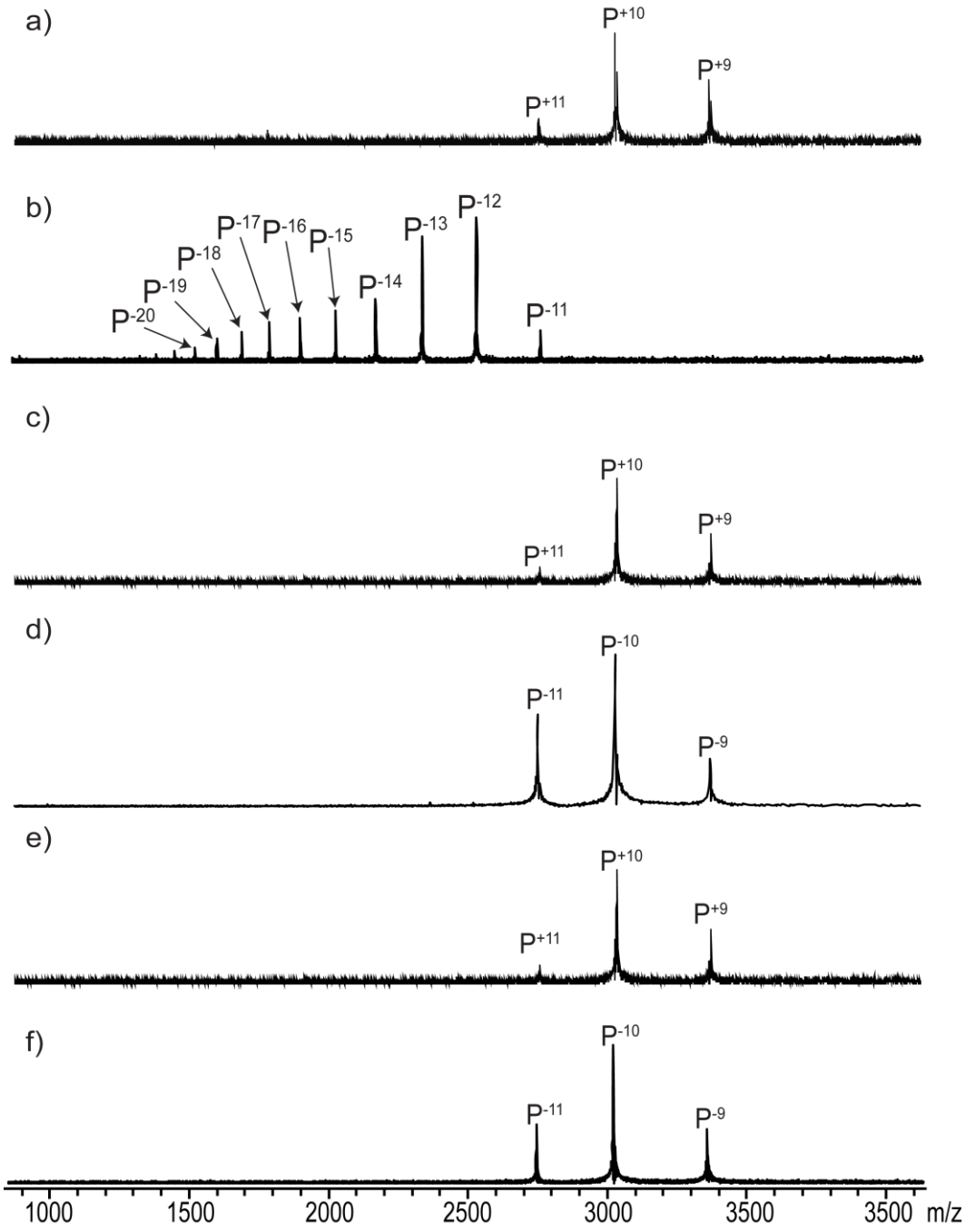

Figure S1: ESI mass spectra acquired in positive mode for aqueous solutions of TcdB-B3C (P, 15 μM) and ammonium acetate (a) 10 mM; average charge state (*ACS*) +9.58, (c) 80 mM; *ACS* +9.81 and (e) 200 mM; *ACS* of +9.91. ESI mass spectra acquired in negative mode for aqueous solutions of TcdB-B3C (P, 15 μM) and ammonium acetate (b) 10 mM; *ACS* -15.11, (d) 80 mM; *ACS* -9.93 and (f) 200 mM; *ACS* -10.01. All measurements carried out using a Bruker Apex II 9.4T FTICR MS.

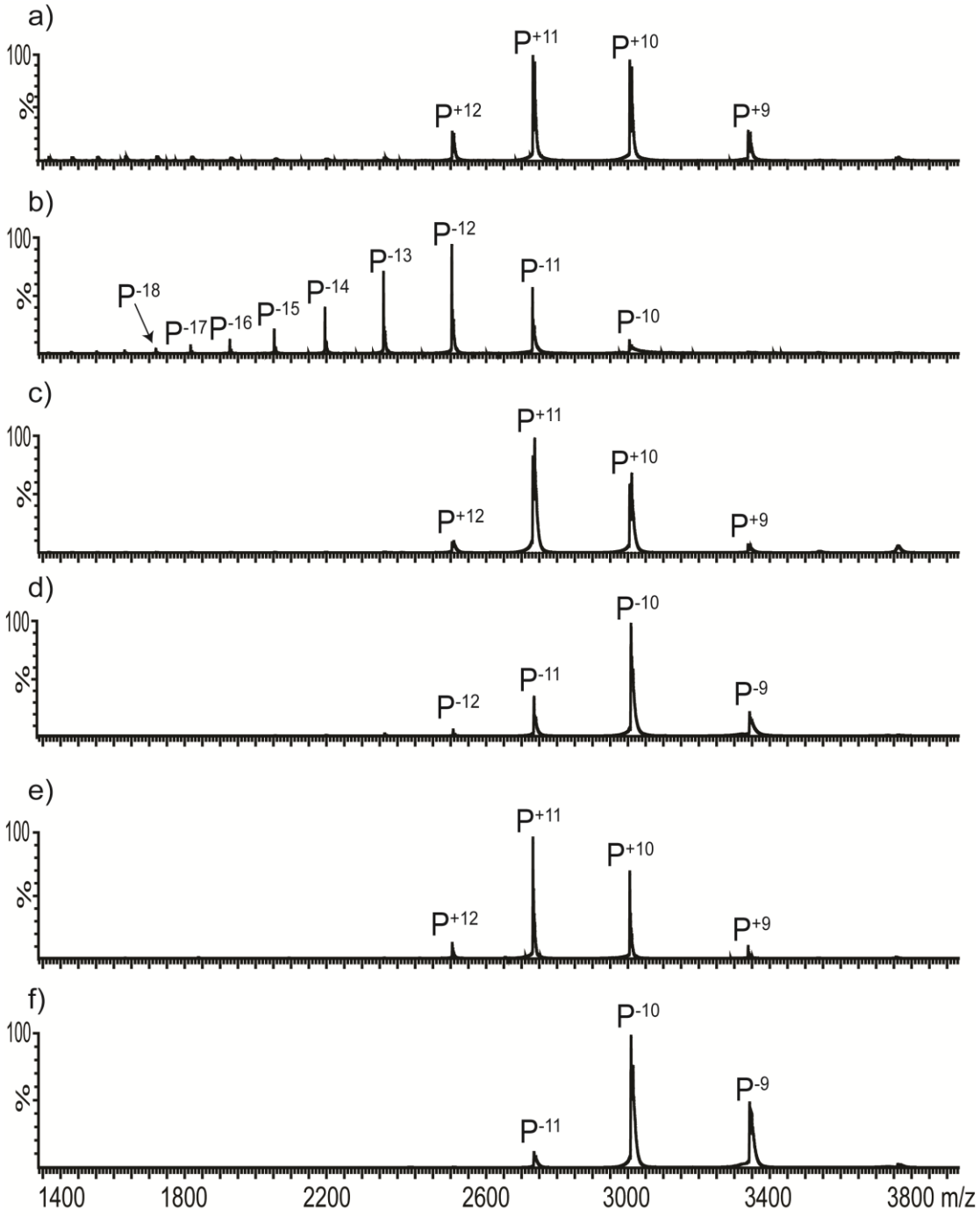

Figure S2: ESI mass spectra acquired for aqueous solutions of TcdB-B4A (P, 15 μM) with 10 mM ammonium acetate in (a) positive mode and (b) negative mode; 60 mM ammonium acetate in (c) positive mode and (d) negative mode; 200 mM ammonium acetate in (e) positive mode and (f) negative mode.

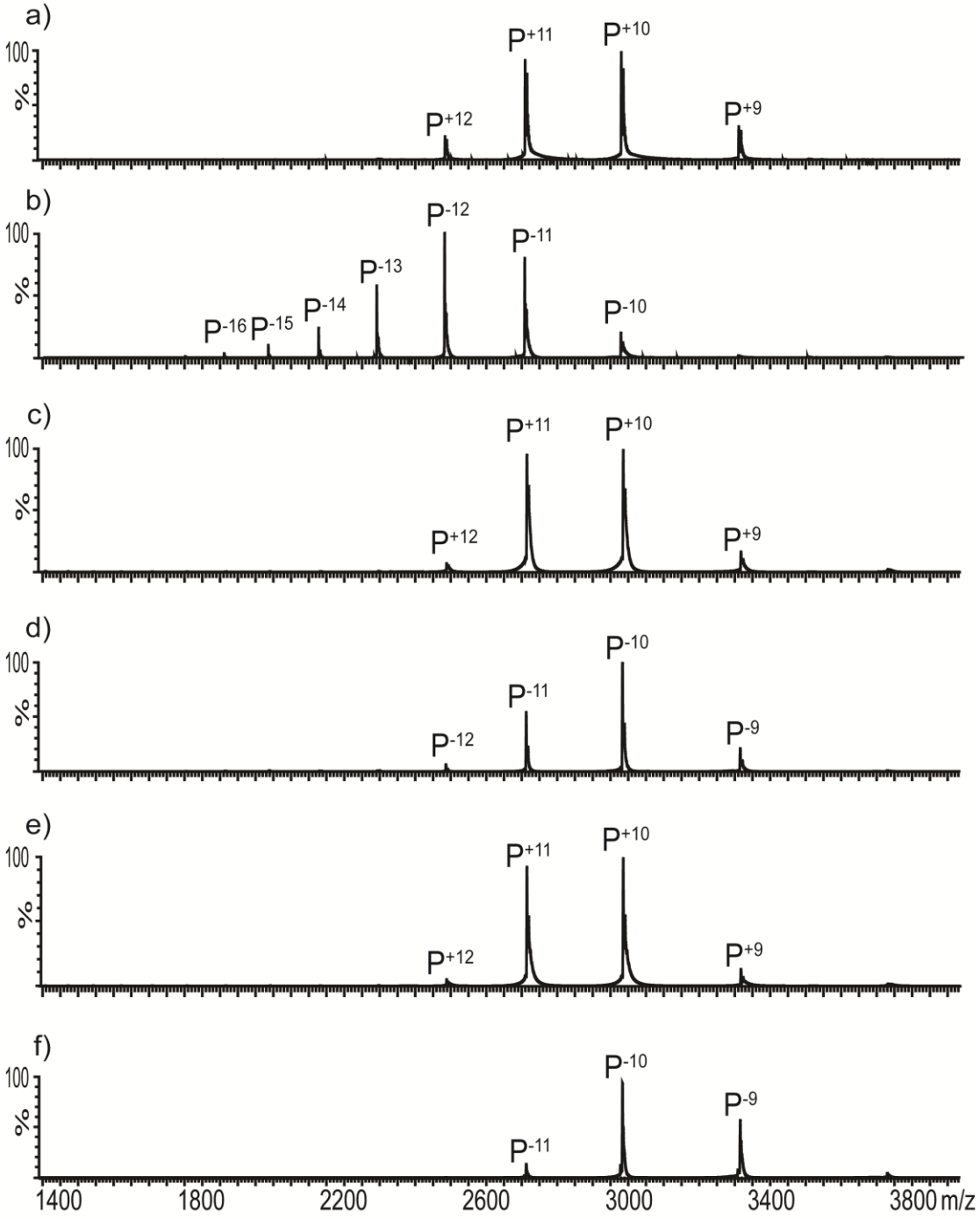

Figure S3: ESI mass spectra acquired for aqueous solutions of TcdB-B4B (P, 15 μM) with 10 mM ammonium acetate in (a) positive mode and (b) negative mode; 40 mM ammonium acetate in (c) positive mode and (d) negative mode; 200 mM ammonium acetate in (e) positive mode and (f) negative mode.

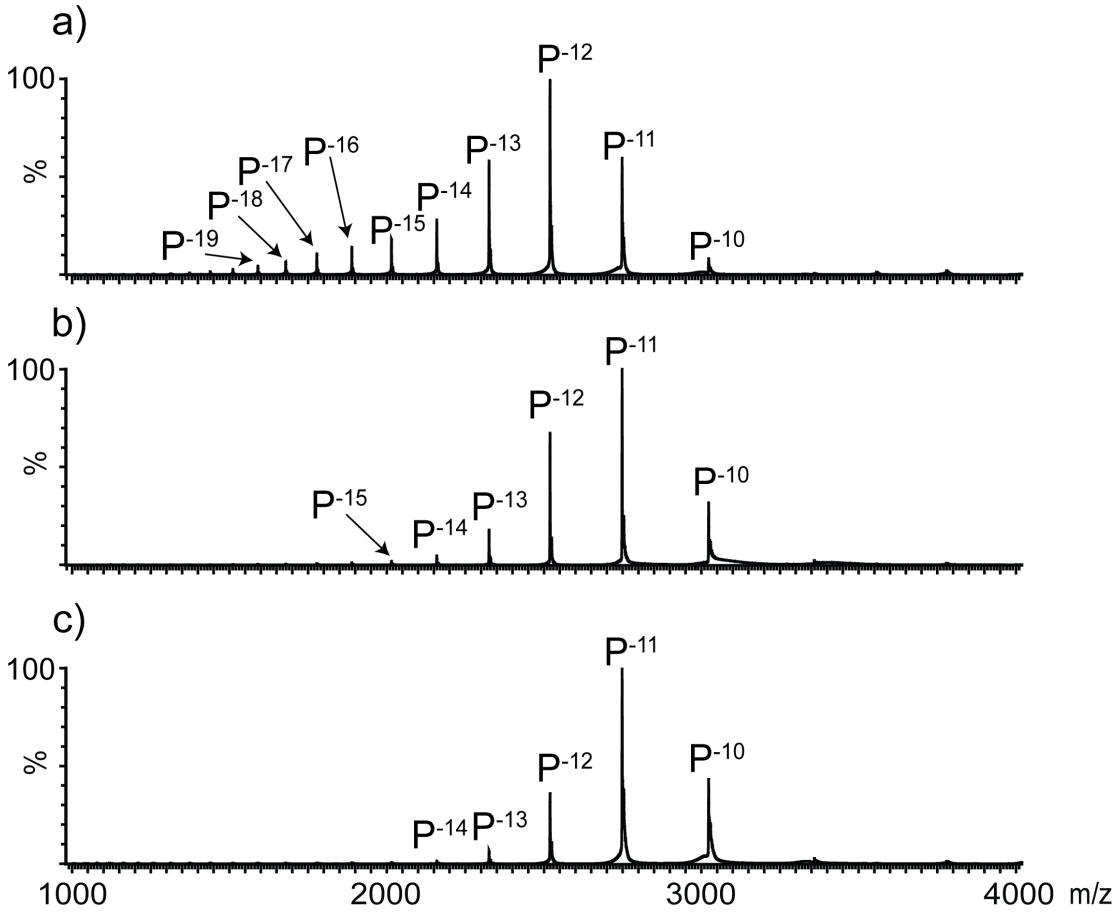

Figure S4: ESI mass spectra acquired for aqueous solutions of TcdB-B3C (P, 15 μM) with (a) 20 mM ammonium acetate; (b) 40 mM ammonium acetate and (c) 60 mM ammonium acetate.

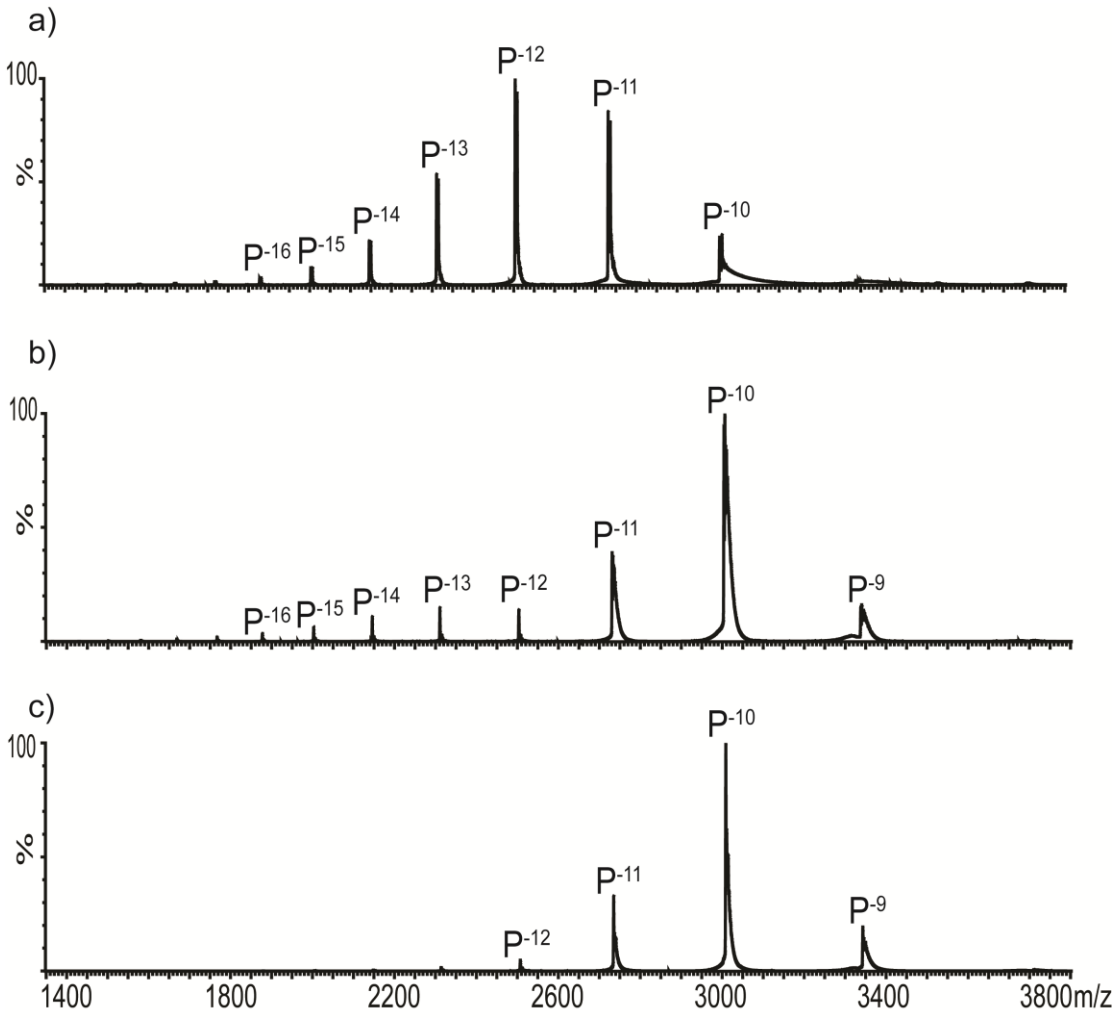

Figure S5: ESI mass spectra acquired for aqueous solutions of TcdB-B4A (P, 15 μM) with (a) 20 mM ammonium acetate; (b) 40 mM ammonium acetate and (c) 60 mM ammonium acetate in negative ion mode.

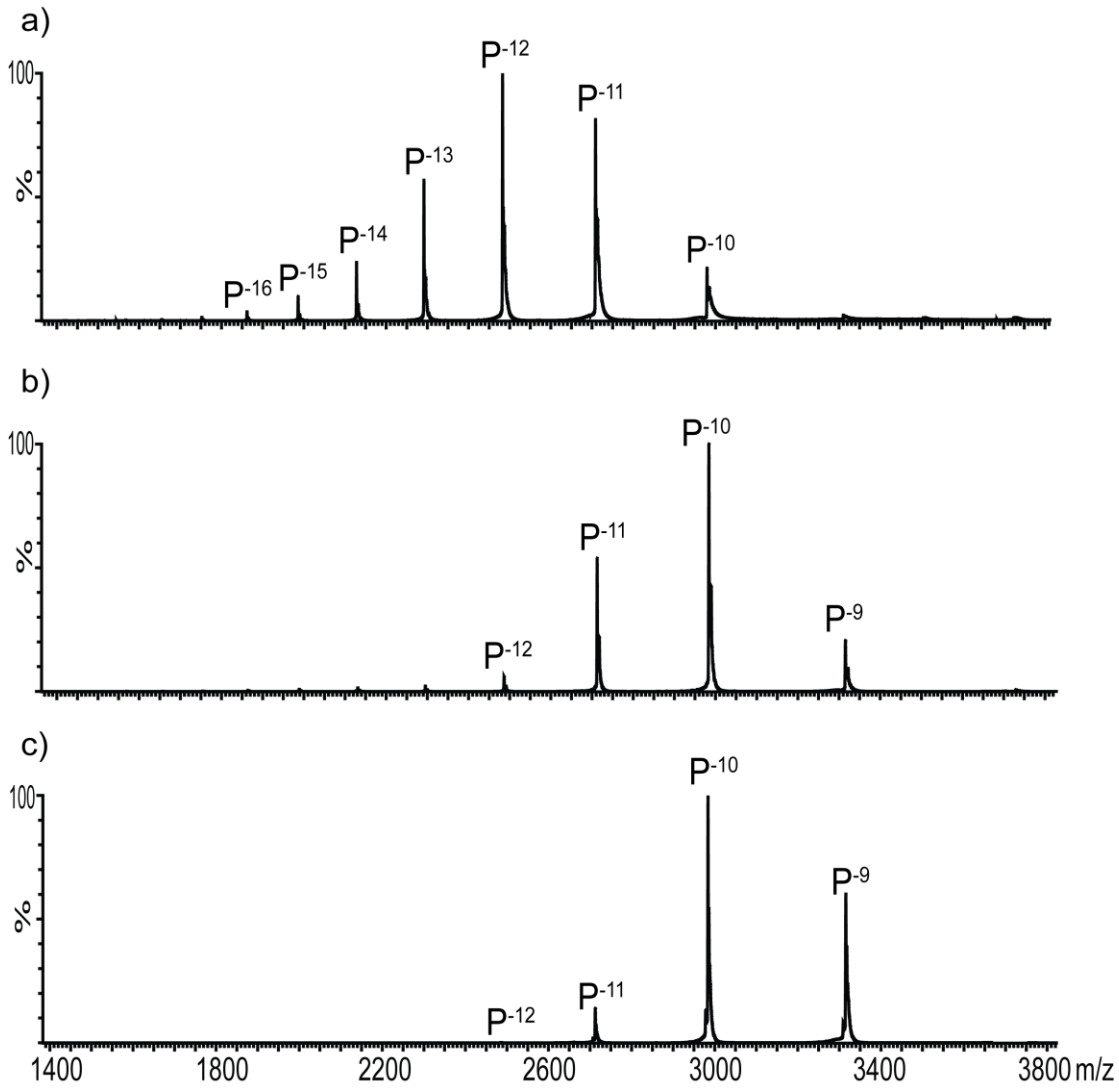

Figure S6: ESI mass spectra acquired for aqueous solutions of TcdB-B4B (P, 15 μM) with (a) 20 mM ammonium acetate; (b) 40 mM ammonium acetate and (c) 60 mM ammonium acetate in negative ion mode.